


 Cite this: *RSC Adv.*, 2025, 15, 45607

A multivariate biosensor for non-invasive glucose and urea monitoring *via* saliva

 Amit Kumar Singh, ^{ab} Shweta Panwar ^b and Sandeep Kumar Jha *^{bc}

Non-communicable diseases such as diabetes and chronic kidney disease (CKD) are major global health concerns due to associated high morbidity rates. Conventional monitoring of these diseases typically involves invasive methods, which can be painful and inconvenient for patients. This study highlights the development of a non-invasive, handheld optical biosensor capable of multivariate analysis using saliva samples. The device used two distinct paper-fluidic strips designed with different enzyme–dye combinations to detect glucose and urea. The biosensor also used ambient temperature compensation to address the differential sensitivity of these sensors owing to variations caused by temperature-dependent enzyme kinetics, thereby enhancing the measurement accuracy. Biosensor characteristics with the glucose oxidase-based strip showed a sensitivity of 1.93 count per mg per dL, linearity range from 8 to 358 mg dL⁻¹, limit of detection (LOD) of 8 mg dL⁻¹, and response time of 7.35 s. The clinical validation shows good correlation between saliva glucose levels (SGLs) and blood glucose levels (BGLs). The urea biosensor strip shows a sensitivity of 1.51 count per mg per dL, LOD of 5 mg dL⁻¹, linearity range from 5 to 90 mg dL⁻¹, and response time of 3 s. The clinical validation for the CKD patient shows a significant correlation between blood urea levels and saliva urea levels. The results demonstrate that the device offers a rapid, reliable, and user-friendly alternative for point-of-care testing (POCT), potentially improving patient compliance and management of diabetes and CKD. *Significance:* The findings suggest that this technology could represent a significant advancement in non-invasive diagnostic tools and can be used as a POCT by chronic patients.

 Received 12th February 2025
 Accepted 12th September 2025

DOI: 10.1039/d5ra01018g

rsc.li/rsc-advances

1 Introduction

Global human health records show that non-communicable ailments, such as heart disease, diabetes, and renal disease, are more predominant than communicable diseases.¹ A World Health Organization (WHO) report states that around 8.5% of the population in 2014 had diabetes.² About 850 million worldwide suffer from kidney disease, mostly in poor countries, lacking diagnosis, prevention, and treatment.³ In the world, around 30 percent of patients with type 1 (juvenile-onset) diabetes and 10–40 percent with type 2 (adult-onset) diabetes may undergo kidney failure, as per a kidney foundation report.⁴ Millions die each year because they do not have access to inexpensive treatments for such non-communicable diseases.⁵ According to some studies, diabetes and chronic kidney disease (CKD) have a significant economic impact on the global gross domestic product (GDP) and expenses.¹ A WHO report suggests that scaling up prevention, strengthening of precautions, and

enhancing disease observations are required by regular monitoring of glucose levels for diabetes^{6,7} and urea for kidney failure⁸ for patients to live a healthy life.

The standard glucose and urea monitoring machines available in the market use invasive and painful measurement techniques, such as using finger-prick-based self-monitoring blood glucose (SMBG) analyzers or inconvenient-to-use wearable patches. Consider a scenario when a chronic diabetic patient has to undergo multiple finger-pricks each day to adjust their insulin dosage. Due to such scenarios, researchers have been exploring the use of different bodily fluids to track chronic diseases. Among these fluids, saliva,^{8,9} urine,^{10,11} sweat,^{12,13} and aqueous humor^{14,15} are available for the non-invasive monitoring of diabetes and CKD. Among these four fluids, saliva is a promising medium because it is easy to collect and handle, as it does not clot,¹⁶ and sample collection is the fastest and most convenient throughout the day among all other body fluids.¹⁷ One of our group's own studies and literature reports show that there is a good correlation of blood glucose⁹ and blood urea nitrogen (BUN)¹⁸ to saliva glucose and saliva urea, respectively. Therefore, it is entirely possible to use saliva-based biosensors for point-of-care technologies (POCT).¹⁹

Various researchers have developed different technologies for POCT-based microfluidic devices that use an

^aDepartment of Biomedical Engineering, Vignan's Foundation for Science Technology & Research, Vadlamudi, Guntur, Andhra Pradesh, 522213, India

^bCentre for Biomedical Engineering, Indian Institute of Technology Delhi, New Delhi 110016, India. E-mail: sandeepjha@cbme.iitd.ac.in

^cDepartment of Biomedical Engineering, All India Institute of Medical Sciences, New Delhi 110029, India



electrochemical, mechanical or optical-based methodology to detect glucose and urea.²⁰ They also find that electrochemical biosensors have some discrepancies, such as the control of ionic concentrations before detection, and the method of strip fabrication is rather complex. In contrast, optical methods require minimal sample preparation, but conventional opto-instrumentation is expensive and requires a complex instrumental set-up. The standard instruments available for multi-analyte detection, e.g., a chemical autoanalyzer use semi-manual methods to detect the analyte type, thus making the instrument not very user-friendly. Amongst the POCT biosensors, Panwar *et al.* reported an optical detection method, which was useful in detecting analytes in saliva samples conveniently, as the medium was semi-transparent,²¹ had less interference with active redox substances,²² and was more reliable and sensitive²³ as compared to electrochemical-based detection. Hence, saliva samples could be used for optical detection of multiple analytes. In optical detection techniques, the latest development is towards mobile phones and surface plasmon resonance (SPR)²⁴ based technologies, of which the latter is costly as well as complex. Our group was amongst the first to validate the use of a smartphone for saliva-based biosensing.^{9,25} Though our earlier efforts were promising, a smartphone-based analyte detection has its own shortcomings, such as continuously changing camera specifications, newer and automatic Android software updates and launch of numerous smartphone models throughout the year, thus making it nearly impossible for developers to keep a track on these modifications as the sensing app is also needed to be revised as per the smartphone as well as Android version. Besides, the mobile phone-based detection method has the issues of ambient light interference and a higher limit of detection (LOD).^{9,25} Besides, the enzymatic reactions driving these POCT or smartphone-based biosensors are dependent on ambient temperature.^{26,27} Duan *et al.* demonstrated the temperature dependence of combined glucose oxidase and peroxidase enzymes for glucose detection in the temperature range of 15–34 °C, which is not good from the POCT perspective, as certain regions in the world experience temperatures beyond this threshold.²⁸

Therefore, to address some of these long-pending problems with POCT and non-invasive biosensing, we have developed a handheld optical system with ambient temperature compensation for multivariate non-invasive sensing. The devices used two distinct paper-fluidic strip types to detect glucose and urea. The instrument automatically detected the strip type inserted for the particular analyte detection, while the enzyme/dye combination was different on each strip. The instrument and strip design were optimized to reduce the LOD and sample volume requirement while increasing the shelf life of the biosensor.²⁹

2 Materials and methods

2.1 Materials

Polyvinyl alcohol (PVA) (cat no. 363138-500G), nitrazine yellow (NY) (cat. no. MKBG8083), glucose oxidase (GOx) (cat. no. SLBS1876V), urease (cat no. SLBT8013-20KU), β -D glucose,

monobasic dihydrogen phosphate, sodium hydroxide pellets (cat. no. 221465), dinitrosalicylic acid (DNS), dibasic monohydrogen phosphate, phenol red (PR) (cat. no. P4161) and the universal indicator (UI) were purchased from Merck (cat no. HX73415675). Dithiothreitol (DTT) (Sigma cat. no. DO632-1G) and filter paper (Whatman: grade-1) used in the biosensor strip development were from Sigma-Aldrich India. Urea (crystalline, extra pure) was purchased from Merck (cat no. HX73415675-100 mL); phenol red (PR) indicator, sodium hypochlorite, and sodium nitroprusside were from Fisher Scientific India. 2-Mercaptoethanol (2-ME) and other acids used were from SRL India.

In the strip fabrication process, the following were used: the Cricut Explore-One model from Cricut, Xerox-color cube 8580 wax printer from Xerox, hotplate from Cole-Parmer stable-temp model no. WW-03407-36, laminating machine from the local market, and PICKit 3 computer programmer from Microchip. All the electronic components used in the optical instrument were from Mouser Electronics, USA. SolidWorks software was used for the 3D design of the chassis, which was manufactured locally. The C18-compiler and MPLABX IDE from Microchip were procured for programming the microcontroller of the instrument.

2.2 Biosensor strip development

Each test strip was a multilayered, paper-based microfluidic device. The base of the strip was a stiff cardstock paper for mechanical support. On top of the base, a strip of Whatman grade 1 filter paper (thickness \sim 330 μ m) was patterned with a hydrophobic wax barrier to define a microfluidic channel (Fig. 1). The wax pattern was designed in CAD software and printed onto the filter paper using a Xerox ColorCube 8580 wax printer. The printed paper was then heated on a hotplate at 120 °C for 120 s to melt the wax and create hydrophobic barriers through the thickness of the paper. The patterned paper strip contained a detection zone (circular, 3.5 mm diameter) where reagents were immobilized, as well as a flow channel (\sim 5 mm length) that guides saliva from the sample application end to the detection zone and helps filter out foam, froth or particulates.

To assemble the strip, the patterned filter paper was sandwiched between a transparent top sheet and a bottom transparent sheet layer, then sealed by a laminating machine. The laminate layers (clear plastic film) provided structural integrity, prevented evaporation, and ensured the sample flows through the defined channel. Each strip design included a secondary circular hole punched through the top laminate and paper layers near the strip's end. This hole served as an identification feature for the instrument: the glucose strip had a 2 mm diameter hole, while the urea strip had a 3 mm diameter hole. When the strip was inserted into the device, an optical sensor read this hole diameter (*via* a LED-LDR pair) to automatically distinguish glucose *vs.* urea strips based on the different light transmission. A small notch in the strip was aligned with a micro-switch in the reader to ensure correct positioning. Fig. 1 illustrates the layered structure of the glucose and urea



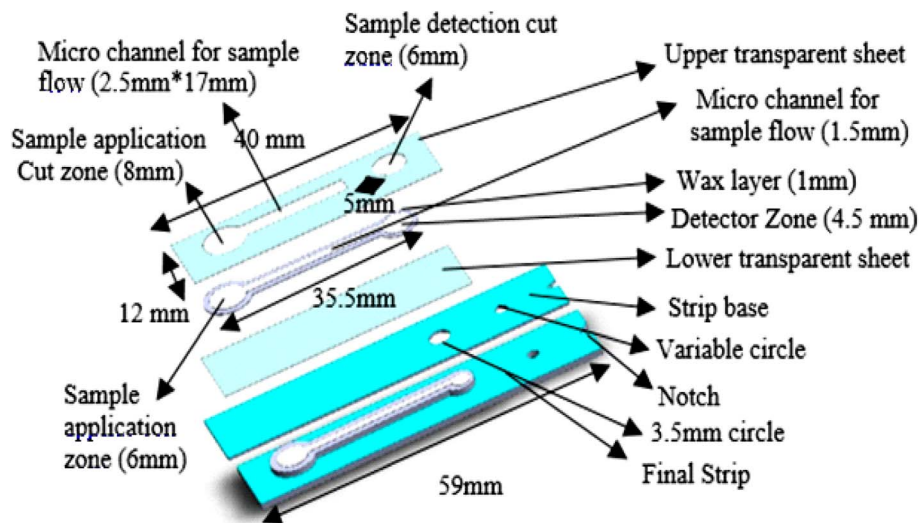


Fig. 1 Biosensor strip design: different layers used for the assembly of glucose and urea biosensor strips.

biosensor strips, with the only variable, circle diameter, different between the strips.

2.3 Immobilization protocol

Glucose biosensor strip. We employed a combined adsorption and polymer entrapment method to immobilize the enzyme and indicator on the detection zone of the paper. A reagent mixture was prepared by first dissolving PVA (0.5% w/v) in 1 mM pH 7.0 phosphate buffer. PVA increases the viscosity to minimize the reagent spread and helps form a film that retains the enzyme and dye in the paper matrix. Next, 0.1% (w/v) NY pH indicator was added to the PVA solution and mixed thoroughly. NY is an azo dye that exhibits a pH-sensitive color change in the microenvironment of the detection zone (blue in alkaline conditions, turning to yellow-green in mildly acidic conditions). Then, glucose oxidase (500 IU per 114 μL of mixture) was added, along with 1 μL of 1.3 M 2-mercaptoethanol (2-ME). The 2-ME acts as a stabilizing agent to prolong the enzyme shelf-life (by preventing sulfhydryl oxidation and preserving enzyme activity). An aliquot of 1.15 μL of this enzyme–dye–polymer mixture was dispensed onto the detection zone of each glucose test strip. The strips were left to dry at room temperature (25 $^{\circ}\text{C}$) in air for about 30 min, then stored at 4 $^{\circ}\text{C}$ in a desiccated container until use.

Glucose sensing mechanism. When a saliva sample is introduced, the glucose in saliva diffuses into the detection zone and is oxidized by immobilized GOx, producing gluconic acid and hydrogen peroxide as by-products. The generation of gluconic acid causes the local pH in the paper strip to drop. The pH-sensitive NY dye responds to this change: under initial neutral-slightly alkaline conditions, the dye is dark blue, but as the pH falls (due to higher glucose concentrations), it transitions to a yellowish-green color (protonated hydrazone form). The degree of color change is concentration-dependent: a higher glucose level produces more acid and thus a greater color shift toward yellow/green. Fig. 2 schematically illustrates the glucose strip reaction and resulting color change after the

reaction at a low glucose concentration (12 mg dL^{-1} , yielding a deep blue color) *versus* a high concentration (262 mg dL^{-1} , yielding a yellow-green color). The optical sensor of the hand-held device detected this colorimetric change quantitatively. In our design, a 620 nm LED (red light) is used to illuminate the detection zone for the glucose assay, and the transmitted light is measured by the color sensor. The choice of 620 nm (which nitrazine yellow strongly absorbs more in its blue form) maximizes sensitivity to the blue-to-yellow transition. In addition to the color sensor reading, the device uses a secondary criterion (light transmittance increases upon wetting) to confirm that saliva has fully reached and covered the detection area before taking a measurement. For blank/reference readings (zero glucose), we used strips prepared identically except that the GOx enzyme was omitted and replaced by an equal protein mass of bovine serum albumin (BSA); these enzyme-free strips do not produce the color change and serve to establish the baseline instrument signal for 0 mg per dL glucose. Estimation of glucose oxidase activity or measurement of salivary glucose concentration was carried out by the standard dinitrosalicylate (DNS) assay.⁹

Urea biosensor strip. A similar approach was used for urea test strips, with adjustments for the different chemistry. The enzyme–dye mixture for urea strips was prepared by dissolving PVA at 1.25% (w/v) in 20 mM pH 7.0 phosphate buffer. Phenol red (PR) indicator was added at 0.1% (w/v) to this solution. PR is an indicator that is yellow-orange under slightly acidic to neutral conditions and turns pinkish-fuchsia in alkaline conditions (pH transition around 6.8–8.2). We then added urease enzyme at 8 IU per 124 μL of mixture, along with 1 μL of 1.3 M 2-ME as stabilizer. An aliquot of 1.25 μL of this urease–PR–PVA mixture was drop-casted onto the detection zone of each urea strip, followed by drying at 25 $^{\circ}\text{C}$ and storage at 4 $^{\circ}\text{C}$ until use (similar to the glucose strips). For calculating the enzyme activity of urease of the urea biosensor strip or to estimate urea in saliva, the standard phenol hypochlorite test (PHT) was followed.³⁰



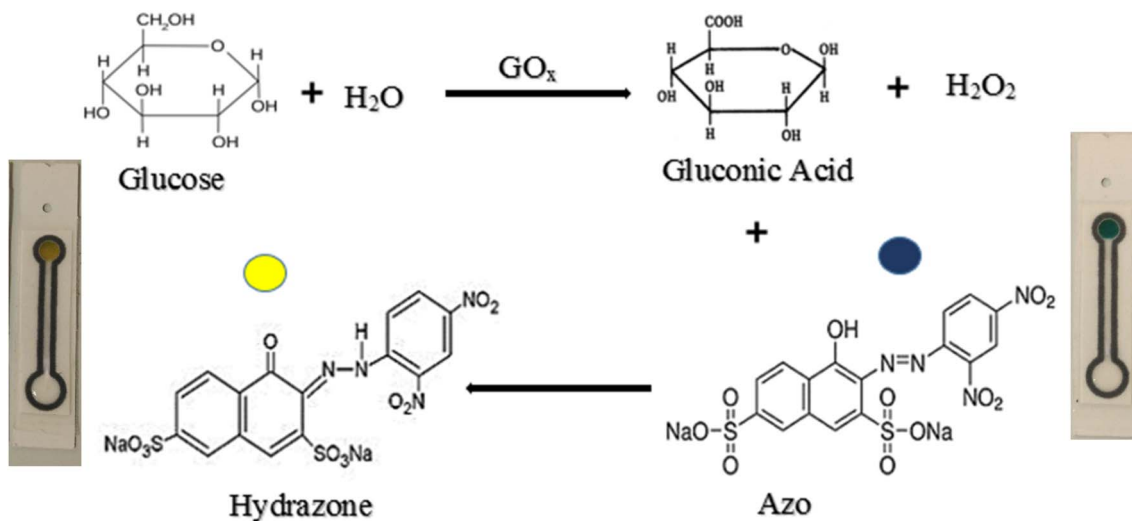


Fig. 2 Schematics of the glucose strip: in the reaction, β -D glucose is converted into gluconic acid in the presence of glucose oxidase (GOD), which induces a color change in nitrazine yellow (NY) from dark blue to yellow. The image on the right shows the glucose biosensor strip tested at 12 mg dL^{-1} , while the image on the left shows the strip tested at 262 mg dL^{-1} .

Urea sensing mechanism. When saliva (which contains urea) is applied, the immobilized urease catalyzes the hydrolysis of urea into NH_3 and CO_2 . The ammonia released raises the local pH in the paper (making it more basic). The PR indicator responds by shifting the color from its acidic form (orange) toward its basic form (pink) as the pH increases. The extent of the color change is proportional to the amount of urea: higher urea concentrations generate more ammonia and thus produce a more pronounced pink color. Fig. 3 depicts the urea strip reaction tested with a low urea level (20 mg dL^{-1} , resulting in a relatively orange color) *versus* a high urea level (120 mg dL^{-1} , resulting in a stronger pink color). In the device, a 530 nm LED (green light) is used for illuminating the detection zone of the urea strip. PR has a noticeable absorbance change in the green

region between its orange and pink states, so the 530 nm source accentuates the measurable change. As with glucose, blank urea strips (with enzyme replaced by BSA) were used to establish the zero baseline.

2.4 Design of an analytical handheld instrument

The handheld instrument consisted of electronic circuitry, battery, display, and a socket to hold the strips in place so that the colorimetric sensor, LED light source and detection zone of the biosensor strips were aligned in such a way that the detector was placed right above the detection zone on the strip and LED under the detection zone at the back side of the strip to allow transmission-based optical detection. The electronic circuit

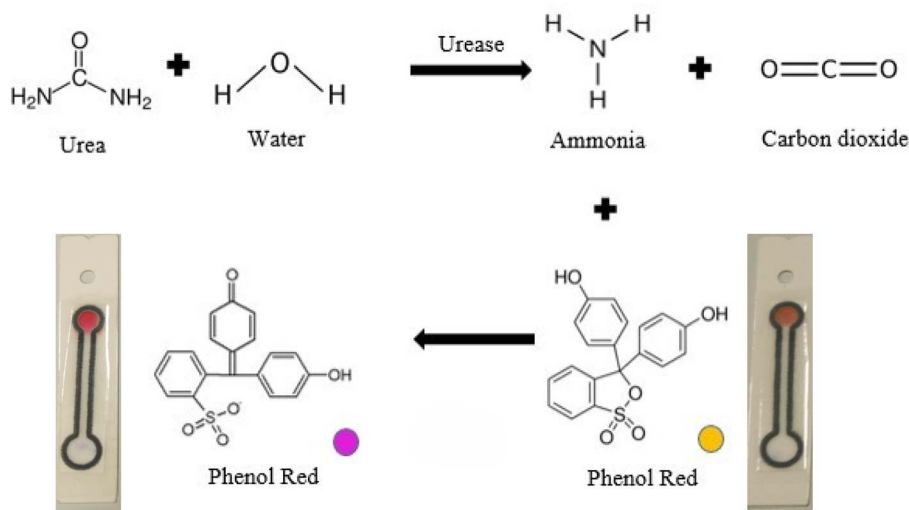


Fig. 3 Schematics of the urea strip: in the reaction, urea is hydrolyzed into ammonia in the presence of urease, resulting in a color change of phenol red (PR) from yellow to pink. The image on the right shows the urea biosensor strip tested at 20 mg dL^{-1} , while the image on the left shows the same strip tested at 120 mg dL^{-1} .



consisted of five essential elements: light source, light detectors, signal processing electronics, Bluetooth, battery, and other electronic parts for data transmission (SI Fig. S1). The circuit design consisted of a red, green, blue (RGB) light-emitting diode (LED) (part no. CLX6B-FKC: consisting of 460–480 nm, 520–540 nm and 619–624 nm peak wavelengths) as a multipurpose light source and a colorimetric sensor S11092 from Hamamatsu, which is highly sensitive among the family of the 16-bit digital color sensor. The colorimetric sensor captured the color change on the strip, and the data was sent to a 16-bit microchip microcontroller (Pic24fj256gb110b) using the I2C protocol. We used a 16-bit family of microcontrollers in our design because the primary data from the color sensor is 16-bit. The detection zone diameter was 3 mm, and the RGB LED cut size was 5.5 mm in diameter to make the overall mechanical alignment of the complete system design conical. The strip contained a notch in its design to ensure a proper fit of the strip into a switch present at the end of the strip chamber. The light-dependent resistor (LDR-1 M Ω) and white LED (SM0805UWC) pair helped identify the strip-type inserted into the instrument, whose resistance changed with the strip type change, due to the difference in diameter of this secondary light-sensing zone. The strip contained the hole specific to the analyte type (2 mm for glucose and 3 mm for urea) aligned with the LDR-light source pair. To measure the biosensor's ambient temperature, we used an onboard temperature sensor (LMT86) in our instrument. The alphanumeric liquid crystal display (LCD) (8 \times 2) used in the device displayed the concentration of the analyte on its screen. The developed instrument also contains a 4GB multi-media card (MMC) to store the patient data and send it to the laptop (Windows) or mobile phones (Android) using Bluetooth technology. For Bluetooth communication, the Bluetooth module was attached to the microcontroller using the Universal Serial Bus (USB) protocol. A BL5C battery was used to power the electronic circuit. Moreover, as some of the electronic components in the instrument ran on a 5 V DC, a 5 V DC converter chip, MCP1253, was added. The rest of the instrument design was the same as the circuit diagram by Singh *et al.*,²⁹ while major alterations were in the form of a detector, light source, strip-type detection module, on-board temperature sensor for 3D biosensor calibration and signal conditioning and transmission protocols. OrCAD software was used in designing the double-sided PCB for the electronic circuitry.

The chassis of the equipment was designed using SolidWorks software and 3D-printed using black colored acrylonitrile-butadiene-styrene (ABS) filament to house the electronic circuitry (SI Fig. S3). The 3D printing method was selected over the mold manufacturing method for chassis manufacturing due to cost and time savings in the prototype development and chassis manufacturing process.

With respect to software development, SI Fig. S4 shows the flowchart of the microcontroller program developed for the biosensor measurement. The microcontroller was initiated to check all the peripherals attached to it for its functionality. Then, it asked the user to insert the strip to be tested. Once the strip was applied, the display showed the analyte name by sensing the strip type inserted, and then asked the user to apply

a saliva sample on the strip. When the sample reached the detection zone within the specified time, the display showed saliva detected; otherwise, it indicated 'saliva scarce', depending on the volume applied by the user. The latter condition ensured that failure of analysis was acknowledged on the device screen and the instrument was returned to the retest mode. After reaching the ample sample volume point, the process moved further and waited for the sample's complete absorption in the detection zone of the strip. For the glucose biosensor strip, the integration time of the colorimetric sensor was kept as 100 ms for 620 nm LED with the 334 ms difference between the two sample points, thus making the scan rate of the strip three times higher as compared to the design by Singh *et al.*,²⁹ which helped in reducing the noise of the measurement due to increase in the scan rate of color sensor. The glucose concentration was calculated for the glucose biosensor strip using SI eqn (1), while for the urea test strip, SI eqn (2) was used. The device could transmit data to the laptop/mobile using Bluetooth technology if required by the user. After the end of measurement, the instrument displayed the data on the LCD and went into sleep mode to save the instrument's power consumption.

2.5 Data analysis

The calibration curve of the developed instrument was obtained using the saliva sample from a healthy donor, which was spiked with a 10% v/v of known concentrations of glucose or urea to obtain higher concentrations. The spiking ratio was restricted to 10% to avoid any significant change in viscosity and other salivary parameters. All biosensor measurements were repeated at least 3 times unless otherwise described, and the sensor response curve was plotted in Origin software using data extracted from the microSD card or through the USB port. The baseline-corrected sensor response at its response time was plotted against the real glucose concentration used, *i.e.*, the intrinsic glucose concentration present in saliva measured through the DNS method and the spiked concentration taken together. Similarly, for urea, the intrinsic concentration was calculated using the phenol hypochlorite method and added to the spiked concentration for plotting the calibration curve. The equation of curves was fed into the device software to automatically calculate the measured BGLs or BUN equivalent on its screen.

2.6 Clinical validation of the biosensor with real samples

All experiments were performed in accordance with the "Indian Council of Medical Research (ICMR) National Ethical Guidelines for Biomedical and Health Research Involving Human Participants (2017)", and approved by the ethics committee at the Indian Institute of Technology, New Delhi (reference number P-018 dated 22-09-2017). Patients were recruited from IIT Delhi Hospital, New Delhi, after getting written consent from them to participate in the clinical trial. To ensure data reliability, patients with poor oral hygiene or dental/gum diseases were excluded from the study.

In order to minimize variations, a standard operating procedure (SOP) was followed for saliva collection. The saliva



sample was collected from the frenulum of the subject's tongue using a medical-grade sterilized cotton ball weighing 33 mg, so that only a 100 μL sample could be collected and transferred to a microcentrifuge tube and later pipetted onto the collection zone of the test strip within 5 minutes of collection. Each sample was collected after the donor rinsed their mouth with drinking water to reduce potential interferences from oral substances like ascorbate and lactate.

3 Results and discussions

3.1 Development of a handheld analytical multi-analyzer device

The interior arrangement of the developed handheld instrument is shown in SI Fig. S2. A white LED and LDR pair helped detect multiple strips made for different analytes by using the secondary hole of varying diameter present on the paper strip. This way, the developed system can be used as a standalone multi-analyzer instrument, albeit by changing the strips for the particular analyte. The instrument was cheaper to fabricate than commercially available multi-analyzer instruments for invasive methods³¹ due to the simplicity of its optical-based design.

The GOx enzyme was optimized at 5 IU per strip for the glucose biosensor and the urease enzyme at 0.08 IU per strip for the urea biosensor to reduce the per-unit strip cost. The phosphate buffer (PB) strength was tested at 1 mM, 10 mM, and 20 mM, and we found that 20 mM PB better controlled the urease enzyme kinetics and helped reduce the enzyme quantity in the assay. Different PVA concentrations were also tested and optimized to improve the color gradient of the biosensor strips by making the immobilization solution viscous to avoid the coffee-ring effect.

The response time of the system was measured as described. We found that once saliva reached the detection zone, the glucose reaction and reading stabilized in about 7.3 s on average. The urea reaction was even faster, taking roughly 3 s to reach a stable endpoint after wetting. These rapid response times are inherent to small diffusion distances in the paper matrix and the high activities of the enzymes at room temperature. It is noteworthy that such quick detection is advantageous for a user-friendly experience, keeping the total testing time (including wicking) under 1–2 minutes. SI Fig. S5 (glucose strip images) and SI Fig. S6 (urea strip images) qualitatively show the color changes after the reactions. It should be mentioned that some very slight color differences at low analyte concentrations might not be distinguishable by the naked eye, but the instrument's sensor accurately quantifies them. This demonstrates the importance of the electronic readout for sensitivity that far exceeded visual observation, especially for near-threshold levels.

3.2 Temperature-compensated response of the biosensor

While the enzyme kinetics of both GOx and urease are affected by ambient temperature and it is not always the case that the sensor measurements are performed by the end-user at

standard 25 °C, very few commercial biosensors, including self-monitoring blood glucometers (SMBG), are actually temperature compensated.³² Nerhus *et al.* have shown the temperature variation of different commercial SMBG in ambient temperature variation.³³ The kinetics of enzymatic reactions are affected at different temperatures, and there are variations in sensor accuracy from winter to summer. During our previous attempts, we observed up to 30% variation in biosensor reproducibility while taking measurements at 4° (winter) (negative error), 25° or 40 °C (summer) (positive error). This effect was mainly due to the fact that GOx stability is retained between pH 4–8 and temperatures 30–60 °C. However, its maximum activity is at 50 °C and not at room temperature,³⁴ at which SMBGs are calibrated. This leads to false elevated readings at temperatures reaching 50 °C and abnormally low readings under cold conditions. This prompted us to move from the standard calibration plot (concentration *vs.* sensor response) to temperature-dependent calibration plots for the glucose biosensor strip (Fig. 4A) for different glucose concentrations ranging from 14–50 °C. While the baseline shown in Fig. 4A was obtained at standard room temperature, 25 °C, we observed that the slope of calibration indeed changed at different temperatures. For this reason, we incorporated a 3D calibration curve considering the difference in slope at different temperatures. An experimental limit of detection (LOD) for the glucose biosensor was determined to be 8 mg dL⁻¹ from Fig. 4A when GOx was substituted for bovine serum albumin (BSA) for immobilization at an ambient temperature of 25 °C. Further, the cutoff sensor count was 1100 using a 620 nm LED light source, with the GOx-dye immobilized strip inserted into the device without the sample, and this value was fed into the device software as the baseline point. Fig. 4B shows the 3D calibration curve for the glucose biosensor while plotting concentration *vs.* sensor response at different temperatures. The calibration equation derived from this plot was used as the basis for the calculation of unknown sample concentrations from the device (SI eqn (S1)) (at *R*-square value of 0.987). The calibration curve was found in the second order for the temperature and the first order for the light intensity change *versus* glucose concentration.

The biosensor parameters calculated showed the glucose biosensor's sensitivity as 1.93 counts per mg per dL, with a LOD of 8 mg dL⁻¹, and linearity range from 8 to 358 mg dL⁻¹ at 25 °C. The response time was 7.35 s. The 3D curve in Fig. 4B and SI eqn (S1) shows that the sensitivity of the glucose biosensor increases with the decrease in ambient temperature. While GOx is a stable enzyme, and we expected a slower enzyme kinetics at lower temperatures, an opposite trend indicates altered dye chemistry at lower temperatures.

Fig. 5A shows the 2D calibration curve of the urea biosensor strip for different urea concentrations at different ambient temperatures ranging from 15–48 °C. LOD of the urea biosensor was calculated as 5 mg dL⁻¹ (Fig. 5A) while urease was substituted with BSA on the strip (at 25 °C). The cutoff sensor count was 2800 using a 530 nm light source, with a urease-dye immobilized strip inserted into the device without the sample and this value was fed into the device software as a baseline point. Fig. 5B shows the 3D calibration curve for the urea



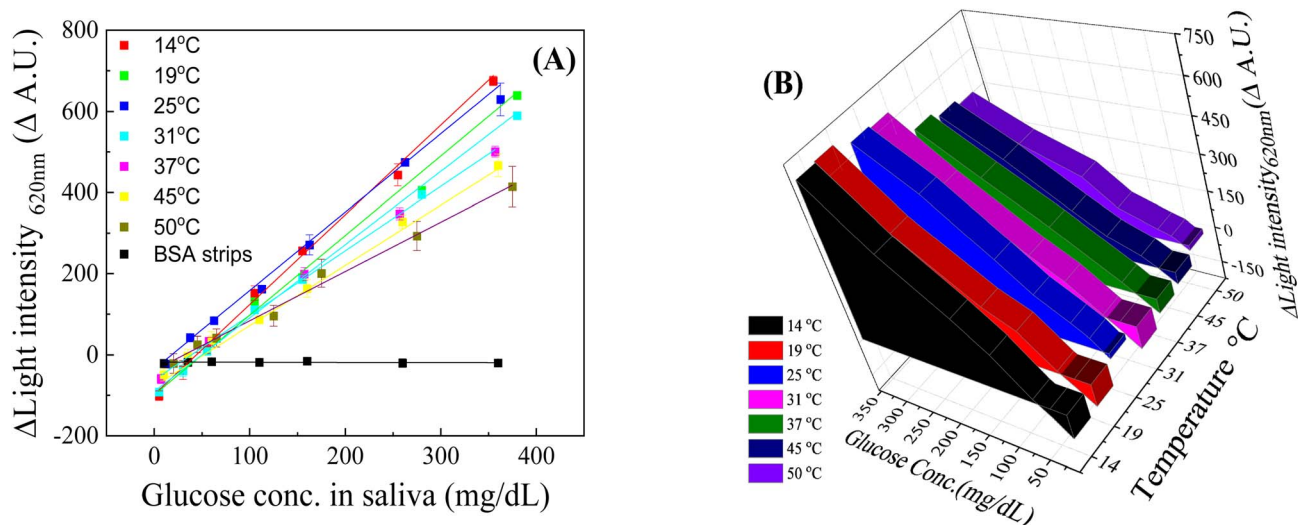


Fig. 4 (A) The 2D-calibration curves at different temperatures show the changes in red color intensity in the detection zone of the strip for different glucose concentrations spiked in saliva at a response time of 7.35 s. (B) 3D calibration curve for the glucose biosensor strip at different ambient temperatures, glucose concentration, and LII for a response time of 7.35 s.

biosensor. SI eqn (S2) shows a fifth-order response for temperature and a fourth-order response for light intensity change versus urea concentration, with an *R*-square value of 0.984. The biosensor parameters calculated showed the sensitivity of the urea biosensor as 1.51 counts per mg per dL, LOD to be 5 mg dL⁻¹, and linearity range from 5 to 90 mg dL⁻¹ at 25 °C. The response time was 3 s. The 3D curve in Fig. 5B and SI eqn (S2) shows that the sensitivity of the urea biosensor increases with the increase in temperature up to 36 °C and then shows a decreasing trend towards 48 °C. The results were in line with reports from other authors^{35,36} and were on expected lines, as urease is not as stable an enzyme as GOx at elevated

temperatures. We first bring the test strips from 4–25 °C and then take the strips to the testing chamber set at the specified temperature.³⁷

3.3 Shelf life and interferent effects on biosensor strips

We compared two enzyme stabilizers, 2-ME and DTT, for enhancing the shelf-life of the strip. Both are known to preserve enzyme activity by maintaining thiol groups. In our tests, strips prepared with 2-ME retained enzyme activity longer than those with DTT, for both GOx and urease strips. This observation was consistent with literature reports; for *e.g.*, Stevens *et al.*³⁸ noted

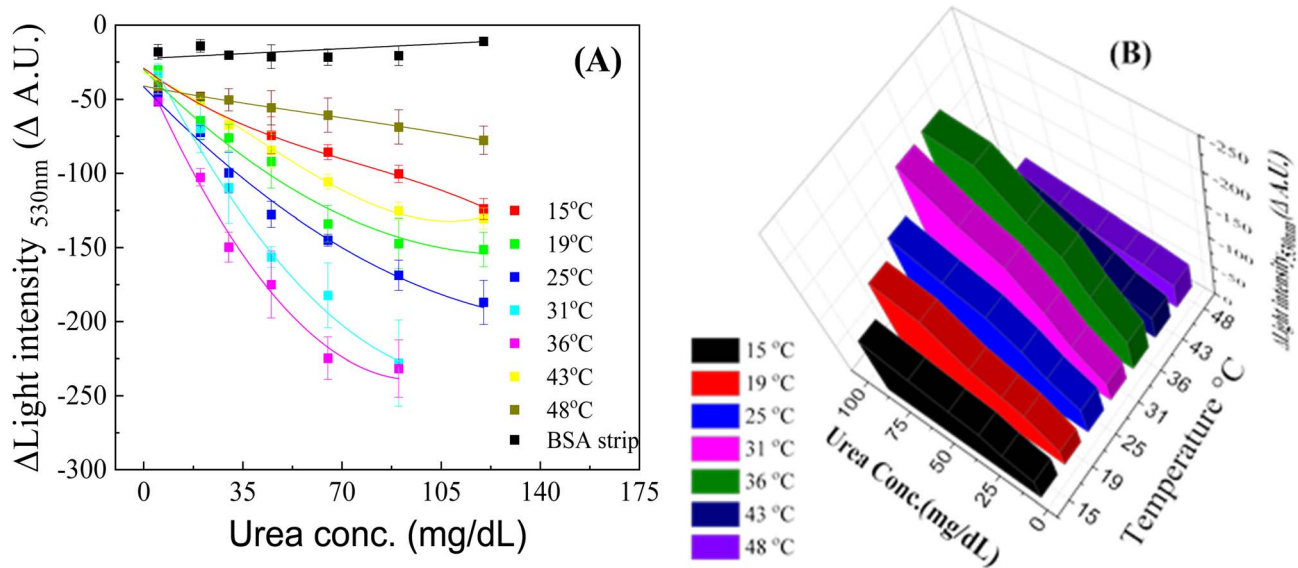


Fig. 5 (A) The 2D-calibration curves at different temperatures show the changes in green color intensity in the detection zone of the strip for different urea concentrations at a response time of 3 s. (B) 3D calibration curve for the urea biosensor strip at different ambient temperatures, urea concentration, and LII for a response time of 3 s.



the effectiveness of 2-ME in stabilizing biosensor enzymes. We performed accelerated aging experiments: strips were stored at room temperature and periodically tested with a standard analyte concentration to monitor any loss of response. SI Fig. S7 and S8 present these stability results. For the glucose strips (SI Fig. S7), the initial sensor reading for 100 mg per dL glucose remained nearly unchanged over multiple weeks when 2-ME was used, whereas strips with DTT showed a gradual decline in signal over time. Similarly, for urea strips tested with 30 mg per dL urea (SI Fig. S8), the 2-ME stabilized strips had superior retention of activity compared to DTT. Based on these findings, 2-ME was selected as the additive in all final formulations. With 2-ME and proper cold storage, the strips demonstrated a shelf-life of at least 2 months with negligible performance degradation, which is quite acceptable for practical use (longer-term stability testing is ongoing). This confirms that while GOx is naturally very stable (often retaining >70–80% activity over 1–2 years when desiccated), urease benefits greatly from the stabilizer as it is less stable at ambient conditions.

As the enzyme activity can be affected by common interferents present in the saliva sample, as illustrated by various authors,³⁹ we performed several tests with common interferents found in the human saliva sample, namely lactic acid (LA), ascorbic acid and urea for glucose strips and LA, NaCl, NH₄Cl, and KCl for urea biosensor strips. SI Fig. S9 and S10 show almost no change in the sensitivity of the two biosensor strips for the biologically present concentrations of common interferents in saliva (0–150 mg dL⁻¹). However, with higher lactic acid concentration, the pH of the microenvironment in the detection zone of the strip was changed, thereby affecting sensor performance. Though anything more than 150 mg per dL lactate accumulation in between tooth gaps may not be practically possible, yet, to avoid this possible interference, we recommend thorough rinsing of mouth and tooth by the end-user with plain water before taking sensor measurements.

For the sample volume variation test, the two biosensor strips were tested by manually placing different aliquots of saliva samples spiked with glucose or urea onto the detection zone directly and it was found that the change in sample volume does not affect the sensor output, as shown in the graph of SI Fig. S11, and the results obtained were better than those reported by Singh *et al.*²⁹ The minimum sample volume requirement at 25 °C was approximately 15 µL in the detection zone of the strip.

3.4 Repeatability test for the analytical instrument

SI Fig. S3 shows the developed instrument, and we used the same methodology to make four identical instruments to check the variability of the biosensing parameters. The repeatability results, obtained using 60 identical blank test strips fabricated using the protocol mentioned in Section 3.2 but devoid of any immobilization and tested on the four developed instruments (15 on each) for sensor count, indicated that the colorimetric sensor of the instrument had a maximum of 1.78% of standard deviation, which was at par with the best industry standard for the instrument design.

3.5 Clinical validation

For clinical validation of the glucose and urea biosensor, testing was performed with strips on 62 subjects who had provided informed consent to participate in the study. The inclusion criteria for glucose saliva tests included healthy controls and diabetic patients aged 18–65 years, and in good physical and mental health. The exclusion criteria for the subjects included those suffering from co-morbidity with hepatic (stomach-related), renal, pulmonary, hematologic diseases, and a history of cardiovascular diseases. The USA Food and Drug Administration approved commercial glucometer from Roche, with the brand name AccuChek Active, was used to correlate the capillary blood glucose levels (BGLs) calculated using it with the saliva glucose levels (SGLs) as measured using our developed biosensor. Secondary correlation was obtained using the conventional DNS assay method. The corresponding SGL values from the developed instrument and DNS method *versus* the BGL values of non-diabetic and diabetic patients were correlated statistically using the Student's *t*-test method. For diabetic subjects under fasting condition (number of subjects = 20), we obtained a *P*-value of 0.07 and 0.06, whereas the Pearson's *R*-value of 0.53 and 0.66 showed a good correlation between BGLs and SGLs from instruments and the DNS method, respectively (Fig. 6A). For diabetic patients under non-fasting condition (random glucose tests) (number of subjects = 17), a *P* value of 0.08 and 0.09 and Pearson's *R* data of 0.49 and 0.47 were obtained, which shows a strong correlation amid BGLs and SGLs from instruments and the DNS method, respectively (Fig. 6B). However, for non-diabetic subjects (fasting condition, *n* = 8), a *P* value of 0.001 and 0.002, and Pearson's *R* data of 0.08 and 0.09 indicated non-substantial correlation amid the two methods (Fig. 6C). Similarly, for non-diabetic subjects (non-fasting condition, *n* = 7), *P* values of 0.002 and 0.001, and Pearson's *R* data of 0.08 and 0.09 indicated non-substantial correlation between the two methods (Fig. 6D).

These outcomes were in agreement with our earlier work performed using a previous version of strips and a meter or a Smartphone camera as a detection element,^{9,25,29} as well as some recent studies carried out using conventional methods.^{40,41} The Clarke error grid analysis results also suggested that all data points lay primarily in the A zone and only a few in the B zone, thereby meeting the ISO 15197:2013 standard of our test.⁴²

For clinical validation of the urea biosensor, the inclusion criteria for urea saliva tests included healthy control subjects and CKD patients aged 18–65 years, who were willing to participate in the study by filling in an informed consent form and were in good physical and mental health. Besides subjects identified with kidney diseases for the past ten years and those who suffered from acute kidney failure, chronic kidney failure, severe nephrotic condition, and glomerulonephritis were included in the study. The exclusion criteria included the patients having a history of nephrotoxic medicine consumption and other systemic diseases, alcohol use, smoking, caffeine consumption through the previous 24 hours, and therapeutic difficulties, except for renal disease and prescription use that



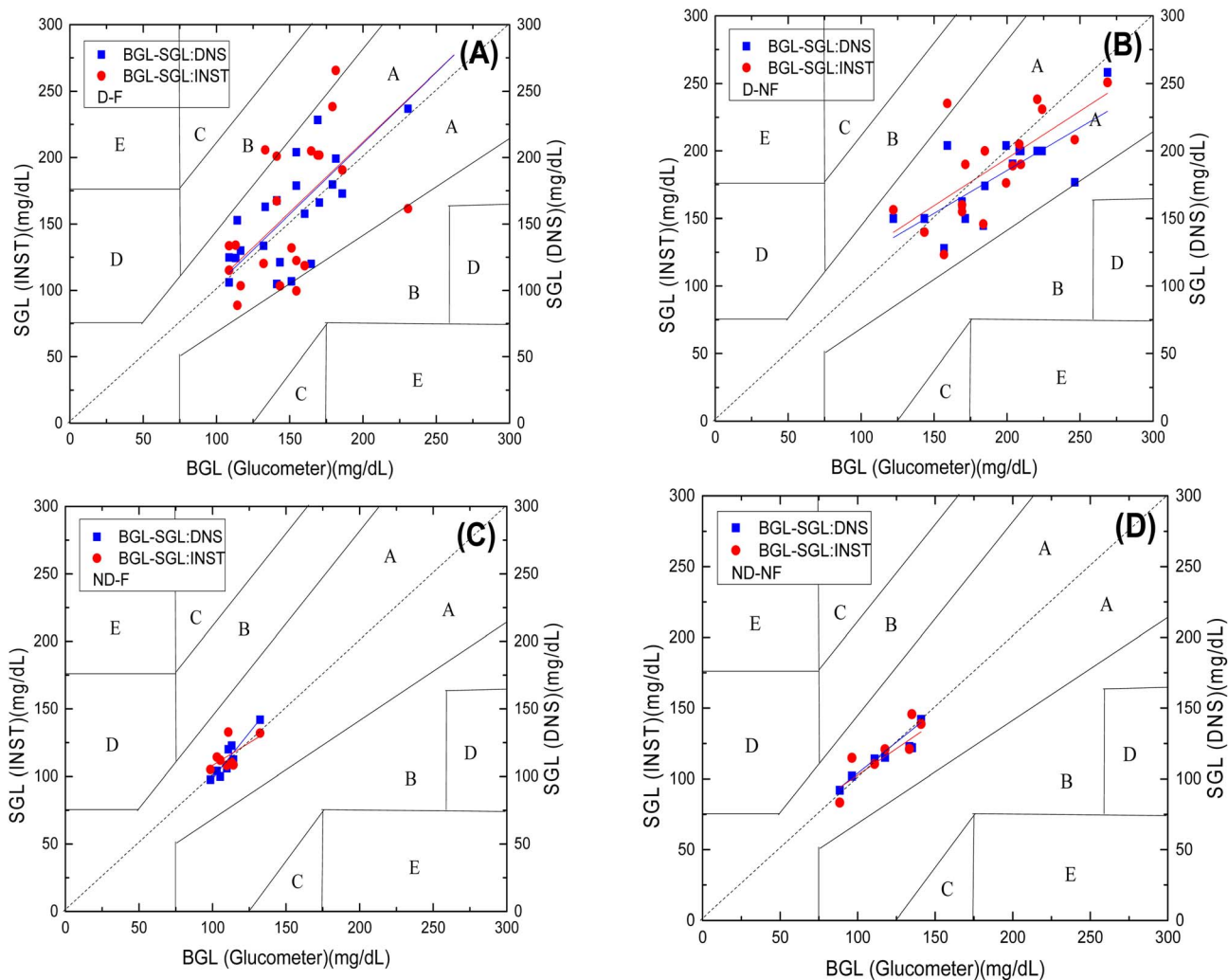


Fig. 6 Clinical validation results (Clarke error grid) for the glucose biosensor: (A) diabetic subjects: pre-breakfast samples, (B) diabetic subjects: post-breakfast samples, (C) non-diabetic subjects: pre-breakfast samples, and (D) non-diabetic subjects: post-breakfast samples.

prejudiced the saliva glands and their secretion. The auto-analyzer instrument model EM-200 from ERBA Diagnostics Mannheim GmbH was used to calculate venous blood urea level

(BUL), and the saliva urea level (SUL) was measured using a developed biosensor and the PHT methods. SUL from the developed instrument and PHT methods *versus* the BUL of CKD

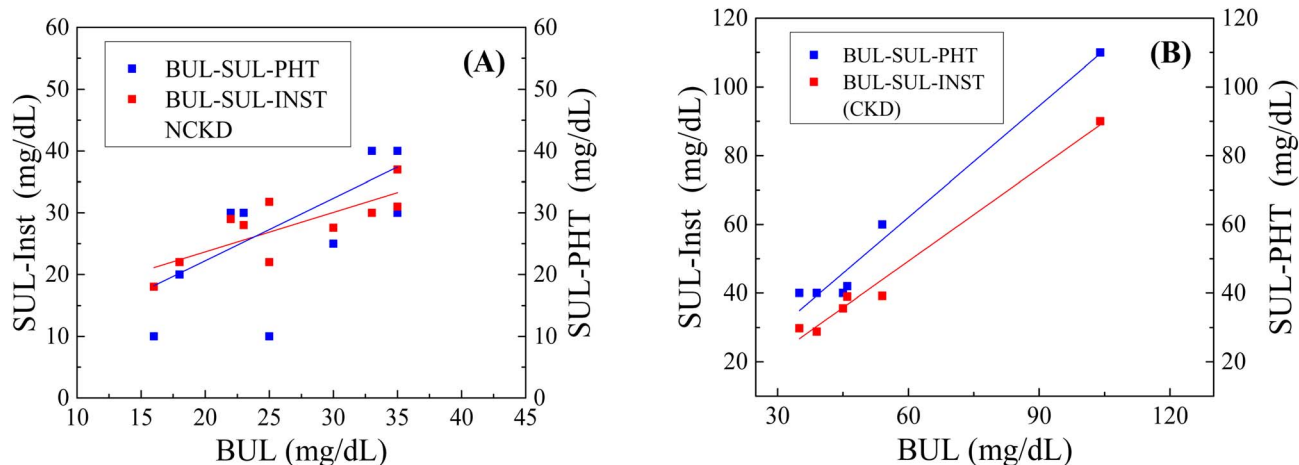


Fig. 7 Clinical validation results for the urea biosensor tested for (A) NCKD and (B) CKD subjects.



and non-chronic kidney disease (NCKD) patients were compared for statistical correlations using the Student's *t*-test method. For NCKD subjects ($n = 10$), we obtained a *P*-value of 0.0002 while having Pearson's *R* data of 0.78 and 0.53, suggesting a significant correlation between BUL to SUL instrument and SUL-PHT readings, respectively (Fig. 7A). Also, for CKD subjects ($n = 6$), a *P* value of 0.46 and 0.24 for BUL to SUL from the developed instrument and SUL-PHT readings, respectively. In contrast, Pearson's *R* data of 0.98 and 0.99 show a significant association between BUL to SUL Instrument and SUL-PHT readings, respectively (Fig. 7B). These outcomes were in agreement with the results of Rhys Evans *et al.*⁴³ for CKD patients, while for NCKD patients, the results were in agreement with those by Soni *et al.*²⁵ The slope of the curve was in the range from 1.08 to 0.64 for the two graphs shown. As Fig. 7 shows, most urea concentration values have an error percentage of 15 from the mean while comparing between the two methods (BUL and SUL); hence, the instrument can still be used for clinical applications, but as the number of subjects tested was very few, we suggest that more samples should be tested for each condition of CKD and NCKD. The LOD of urea test strips must also be improved on the developed instrument to get better accuracy at lower SUL values.

4 Conclusions

We have demonstrated a point-of-care handheld optical biosensor that can non-invasively measure glucose and urea from saliva, with built-in compensation for ambient temperature variation. The system comprises disposable paper-based strips for each analyte and a reusable electronic reader. The strips utilize enzyme-catalyzed reactions (glucose oxidase and urease) coupled with pH-sensitive color indicators to produce a concentration-dependent color change, which is quantified by the reader's color sensor. Key performance metrics achieved include low limits of detection (8 mg dL^{-1} for glucose and 5 mg dL^{-1} for urea in saliva), wide linear ranges covering normoglycemic to hyperglycemic levels and normal to uremic levels, and fast analysis times ($\sim 3\text{--}7 \text{ s}$ after sample introduction). The device's automatic temperature calibration feature distinguishes it from many prior devices, ensuring accuracy across a broad range of environmental conditions without user intervention. In practical validation with human subjects, the saliva glucose readings from the device showed good correlation with blood glucose for diabetic patients (though, as expected, not in healthy individuals at low concentrations), and saliva urea readings closely tracked blood urea levels, especially in CKD patients. These results confirm that the biosensor can provide clinically relevant information non-invasively.

The technology presented could improve chronic disease management by enabling patients to monitor their health markers more comfortably and frequently. For diabetics, a saliva-based test could supplement blood glucometer readings or serve as a screening tool when blood testing is not feasible. For renal patients, saliva urea testing might allow quick checks of uremic status between laboratory visits. The device's portable and user-friendly design makes it suitable for point-of-care

settings, home self-testing, or use in resource-limited areas where laboratory infrastructure is lacking. Moreover, the modular strip approach means additional saliva analytes (ketones, cortisol, *etc.*) could potentially be incorporated in the future, expanding the diagnostic scope of the device.

This study represents an initial evaluation, and certain limitations should be acknowledged. The sample size for clinical validation was modest (especially for CKD patients, $n = 6$); larger studies are needed to fully establish the diagnostic accuracy of the device and reproducibility in diverse populations. Saliva composition can be influenced by factors such as hydration, circadian rhythms, diet, and oral health, which may introduce variability – these factors will need further investigation. In its current form, the device provides one analyte result per strip; while the system is multi-analyte in that it can handle different strips, it does not measure multiple analytes simultaneously on a single strip. In the future, integrating multiple test zones on one strip or using multiplexed sensor arrays could be explored. Another limitation is that for normoglycemic healthy individuals, saliva glucose is often below the detection threshold, which means the device is most beneficial for detecting hyperglycemia rather than for fine monitoring at low concentrations. This is an inherent limitation of saliva as a medium (not a limitation of the device), but it means the utility in the euglycemic range is limited.

Going forward, we aim to refine the biosensor and address the above limitations. First, we plan to conduct extensive clinical testing with larger cohorts to gather statistical strength on sensitivity and specificity for conditions like diabetes and CKD. We will also investigate longitudinal tracking of patients to see how well saliva readings predict changes in blood readings over time. Second, improvements in the sensor algorithm will be explored – for instance, implementing machine learning on the color sensor outputs to possibly correct for any salivary matrix effects beyond pH, or to detect anomalous readings. Third, to expand the panel of detectable analytes, we will prototype strips for additional biomarkers relevant to metabolic health (such as uric acid for gout/kidney health, or saliva ketone monitoring for diabetic ketoacidosis risk). The device hardware already supports multi-wavelength sensing, which could facilitate those additions.

In conclusion, this work presents a promising step towards non-invasive, multi-analyte point-of-care diagnostics. By uniting chemical sensing principles with innovative engineering (temperature compensation, auto strip recognition), we achieved a level of performance that approaches standard blood-based assays for two important analytes. The technology holds potential to improve patient compliance and enable broader screening of chronic conditions. With further development and validation, such saliva-based biosensors could become valuable tools in the healthcare arsenal for managing diabetes, kidney disease, and beyond.

Ethical statement

The Institute Ethical Committee approved the protocol (reference number IEC-P-018 dated 22-09-2017).



Conflicts of interest

No conflict of interest.

Data availability

Supplementary information: supplementary figures and equations. See DOI: <https://doi.org/10.1039/d5ra01018g>.

Acknowledgements

Writers are grateful to the Indian Institute of Technology, Delhi, for providing amenities, set-up, and in-house economic provision for the work. The work has been patented as Jha & Singh, 2019 (granted): a biosensor for detecting multi analyte in oral fluid. Indian Patent No. 359606 (IN201811021813A), filed 11-6-2018, published 10-06-2019; and PCT No. WO2019239427A1 (PCT/IN2019/050443), filed 10-6-2019, publication date 19-12-2019. Any commercial exploitation of this work is prohibited, and the technology can be licensed through the Foundation for Innovation and Technology Transfer, Indian Institute of Technology, Delhi, India. However, academic progression of work is permitted under the fair use doctrine.

References

- W. G. Couser, G. Remuzzi, S. Mendis and M. Tonelli, The contribution of chronic kidney disease to the global burden of major noncommunicable diseases, *Kidney Int.*, 2011, **80**, 1258–1270.
- W. H. Organisation, *Global Action Plan on the Public Health Response to Dementia 2017–2025*, Geneva World Heal. Organ., 2017, vol. 52.
- A. Francis, M. N. Harhay, A. C. M. Ong, S. L. Tummalapalli, A. Ortiz, A. B. Fogo, D. Fliser, P. Roy-Chaudhury, M. Fontana, M. Nangaku, C. Wanner, C. Malik, A. Hradsky, D. Adu, S. Bavanandan, A. Cusumano, L. Sola, I. Ulasi, V. Jha, A. S. of Nephrology, E. R. Association and I. S. of Nephrology, Chronic kidney disease and the global public health agenda: an international consensus, *Nat. Rev. Nephrol.*, 2024, **20**, 473–485.
- A. Guiseppi-Elie, Electroconductive hydrogels: synthesis, characterization and biomedical applications, *Biomaterials*, 2010, **31**, 2701–2716.
- J. W. Wang and E. T. Lee, *Statistical Methods for Survival Data Analysis*, Wiley, New York, 3rd edn, 2003.
- A. Takian and S. Kazempour-Ardebili, Diabetes Dictating Policy: An Editorial Commemorating World Health Day 2016, *Int. J. Health Policy Manag.*, 2016, **5**, 571–573.
- J. R. Anusha, H.-J. Kim, A. T. Fleming, S. J. Das, K.-H. Yu, B. C. Kim and C. J. Raj, Simple fabrication of ZnO/Pt/chitosan electrode for enzymatic glucose biosensor, *Sens. Actuators, B*, 2014, **202**, 827–833.
- A. Soni and S. K. Jha, Saliva based noninvasive optical urea biosensor, in *2017 IEEE Sensors*, 2017, pp. 1–3.
- A. Soni and S. K. Jha, A paper strip based non-invasive glucose biosensor for salivary analysis, *Biosens. Bioelectron.*, 2015, **67**, 763–768.
- M. Alqasameh, L. Y. Heng, M. Ahmad, A. S. S. Raj and T. L. Ling, A Large Response Range Reflectometric Urea Biosensor Made from Silica-Gel Nanoparticles, *Sensors*, 2014, **14**, 13186–13209.
- S. Geetha and V. Lakshminarayanan, An Artificial Intelligence Based Glucometer for Diabetic Patients using Urinal Analysis, *Bonfring Int. J. Power Syst. Integr. Circuits*, 2013, **3**, 1–6.
- R. D. Munje, S. Muthukumar and S. Prasad, Lancet-free and label-free diagnostics of glucose in sweat using zinc oxide based flexible bioelectronics, *Sens. Actuators, B*, 2017, **238**, 482–490.
- E. K. Varadharaj and N. Jampana, Non-Invasive Potentiometric Sensor for Measurement of Blood Urea in Human Subjects Using Reverse Iontophoresis, *J. Electrochem. Soc.*, 2016, **163**, B340–B347.
- T. Stachon, A. Stachon, U. Hartmann, B. Seitz, A. Langenbucher and N. Szentmáry, Urea, Uric Acid, Prolactin and fT4 Concentrations in Aqueous Humor of Keratoconus Patients, *Curr. Eye Res.*, 2017, **42**, 842–846.
- J. Zhang, W. Hodge, C. Hutnick and X. Wang, Noninvasive diagnostic devices for diabetes through measuring tear glucose, *J. Diabetes Sci. Technol.*, 2011, **5**, 166–172.
- S. Baliga, S. Muglikar and R. Kale, Salivary pH: a diagnostic biomarker, *J. Indian Soc. Periodontol.*, 2013, **17**, 461–465.
- F. Ahmadi-Motamayel, M. T. Goodarzi, S. S. Hendi, H. Abdolsamadi and N. Rafeian, Evaluation of salivary flow rate, pH, buffering capacity, calcium and total protein levels in caries free and caries active adolescence, *J. Dent. Oral Hyg.*, 2013, **5**, 35–39.
- E. M. L. Cardoso, A. L. Arregger, O. R. Tumilasci, A. Elbert and L. N. Contreras, Assessment of salivary urea as a less invasive alternative to serum determinations, *Scand. J. Clin. Lab. Invest.*, 2009, **69**, 330–334.
- M. Yamaguchi, Salivary Sensors in Point-of-Care Testing, *Sensor. Mater.*, 2010, **22**, 143–153.
- N. M. M. Pires, T. Dong, U. Hanke and N. Hoivik, Recent developments in optical detection technologies in lab-on-a-chip devices for biosensing applications, *Sensors*, 2014, **14**, 15458–15479.
- S. Panwar, P. Sarkar, D. S. Kasim, R. Anand, A. Priya, S. Prakash and S. K. Jha, Portable optical biosensor for point-of-care monitoring of salivary glucose using a paper-based microfluidic strip, *Biosens. Bioelectron.: X*, 2024, **17**, 100452.
- S. K. Jha, M. Kanungo, A. Nath and S. F. D'Souza, Entrapment of live microbial cells in electropolymerized polyaniline and their use as urea biosensor, *Biosens. Bioelectron.*, 2009, **24**, 2637–2642.
- J. Kumar, S. K. Jha and S. F. D'Souza, Optical microbial biosensor for detection of methyl parathion pesticide using *Flavobacterium* sp. whole cells adsorbed on glass fiber filters as disposable biocomponent, *Biosens. Bioelectron.*, 2006, **21**, 2100–2105.



- 24 R. Verma and B. D. Gupta, A novel approach for simultaneous sensing of urea and glucose by SPR based optical fiber multianalyte sensor, *Analyst*, 2014, **139**, 1449–1455.
- 25 A. Soni and S. K. Jha, Smartphone based non-invasive salivary glucose biosensor, *Anal. Chim. Acta*, 2017, **996**, 54–63.
- 26 E. Odebunmi and S. Owalude, Kinetic And Thermodynamic Studies Of Glucose Oxidase Catalysed Oxidation Reaction of Glucose, *J. Appl. Sci. Environ. Manag.*, 2007, **11**(4), 95–100.
- 27 B. Krajewska, R. van Eldik and M. Brindell, Temperature- and pressure-dependent stopped-flow kinetic studies of jack bean urease. Implications for the catalytic mechanism, *JBIC, J. Biol. Inorg. Chem.*, 2012, **17**, 1123–1134.
- 28 W. Duan, J. Cheng and J. Guo, Smartphone-based photochemical sensor for multiplex determination of glucose, uric acid, and total cholesterol in fingertip blood, *Analyst*, 2022, **147**(14), 3285–3290.
- 29 A. K. Singh and S. K. Jha, Fabrication and Validation of a Handheld Non-Invasive, Optical Biosensor for Self-Monitoring of Glucose Using Saliva, *IEEE Sens. J.*, 2019, **19**, 8332–8339.
- 30 M. W. Weatherburn, Phenol-hypochlorite reaction for determination of ammonia, *Anal. Chem.*, 1967, **39**, 971–974.
- 31 C. Scully, J. V. Bagan, C. Hopper and J. B. Epstein, Oral cancer: current and future diagnostic techniques, *Am. J. Dent.*, 2008, **21**, 199–209.
- 32 G. A. Hayter, D. M. Bernstein, M. J. Fennell, M. R. Love, K. J. Doniger, S. Zhang, M. K. Sloan, H. Cho, T. J. Kunich, J.-P. Cole, C. A. Thomas, E. S. Budiman, D. L. Li, R. Cheng and U. Hoss, Temperature-compensated analyte monitoring devices, systems, and methods thereof, *EP Pat.*, EP4122384A1, International product patent, 2023.
- 33 K. Nerhus, P. Rustad and S. Sandberg, Effect of ambient temperature on analytical performance of self-monitoring blood glucose systems, *Diabetes Technol. Ther.*, 2011, **13**, 883–892.
- 34 Y. Guo, F. Lu, H. Zhao, Y. Tang and Z. Lu, Cloning and heterologous expression of glucose oxidase gene from *Aspergillus niger* Z-25 in *Pichia pastoris*, *Appl. Biochem. Biotechnol.*, 2010, **162**, 498–509.
- 35 A. K. Smith, P. A. Belter and R. L. Anderson, Urease activity in soybean meal products, *J. Am. Oil Chem. Soc.*, 1956, **33**, 360–363.
- 36 S. Harrita, V. Priya V and R. Gayathri, Assessment of urease activity in soya bean products, *Drug Invent. Today*, 2018, **10**, 2045–2047.
- 37 N.-S. Choi, J.-H. Hahm, P. J. Maeng and S.-H. Kim, Comparative study of enzyme activity and stability of bovine and human plasmins in electrophoretic reagents, beta-mercaptoethanol, DTT, SDS, Triton X-100, and urea, *J. Biochem. Mol. Biol.*, 2005, **38**, 177–181.
- 38 R. Stevens, L. Stevens and N. C. Price, The stabilities of various thiol compounds used in protein purifications, *Biochem. Educ.*, 1983, **11**, 70.
- 39 K. Ngamchuea, K. Chaisiwamongkhol, C. Batchelor-McAuley and R. G. Compton, Chemical analysis in saliva and the search for salivary biomarkers – a tutorial review, *Analyst*, 2018, **143**, 81–99.
- 40 L. Shettigar, S. Sivaraman, R. Rao, S. A. Arun, A. Chopra, S. U. Kamath and R. Rana, Correlational analysis between salivary and blood glucose levels in individuals with and without diabetes mellitus: a cross-sectional study, *Acta Odontol. Scand.*, 2024, **83**, 101–111.
- 41 L. Vuletić, S. Špalj, D. Rogić and K. Peroš, The rise in glucose concentration in saliva samples mixed with test foods monitored using a glucometer: an observational pilot study, *J. Oral Biosci.*, 2019, **61**, 201–206.
- 42 S. Sengupta, A. Handoo, I. Haq, K. Dahiya, S. Mehta and M. Kaushik, Clarke Error Grid Analysis for Performance Evaluation of Glucometers in a Tertiary Care Referral Hospital, *Indian J. Clin. Biochem.*, 2022, **37**, 199–205.
- 43 R. Evans, V. Calice-Silva, J. G. Raimann, U. Hemmila, A. Craik, M. Mtekatoka, F. Hamilton, Z. Kawale, H. Dobbie, G. Dreyer, N. Levin, P. Kotanko and R. Pecoits-Filho, Diagnostic Performance of a Saliva Urea Nitrogen Dipstick to Detect Kidney Disease in Malawi, *Kidney Int. Rep.*, 2017, **2**, 219–227.

